# Geotechnical and Geophysical Characterization of a Tailings Dam Facility using Machine Learning Techniques

Fernanda Matarazo<sup>1</sup>, Craig Christensen<sup>2</sup>, Fernando Pacheco<sup>3</sup>, Priscila Rodrigues<sup>3</sup>, Flora Cezimbra<sup>1</sup> and Víctor Rocha<sup>1</sup>

- 1. Vale, Brazil
- 2. EMerald Geomodelling, Norway
- 3. EMerald Geomodelling, Brazil

## **ABSTRACT**

This study presents an integrated geotechnical and geophysical approach for characterizing tailings within a tailings dam asset in Brazil's Iron Quadrangle. The objective was to delineate key subsurface interfaces and classify tailings materials using a combination of airborne electromagnetic (AEM) data, ground-based geophysical surveys, and geotechnical borehole information, supported by machine learning techniques. The methodology involved two main modeling workflows: interface modeling using artificial neural networks to predict the depth of geological boundaries (e.g., base of soft soil, natural terrain, base of tailings, base of residual soil, and phreatic surface), and volumetric classification using a random forest to estimate the spatial distribution of different types of tailings. Predictive models were trained using supervised learning, using target values derived mainly from geotechnical soundings and support by features from AEM resistivity and magnetic susceptibility models, spatial coordinates, and terrain indices. Prediction uncertainty was estimated in all models. Results showed that the AEM-based models effectively captured large-scale subsurface trends, particularly for the natural terrain and base of tailings. The residual soil and soft soil models exhibited higher uncertainty due to limited resolution, signal attenuation in the deepest portions of the tailings and sparse training data. Volumetric classification identified fine tailings as the dominant material, with coarse and transitional tailings occurring in specific zones. A separate model distinguished contractive and dilative tailings behavior, with good predictive performance. Challenges included the limited vertical resolution of the AEM system, temporal mismatches between datasets, and subjectivity in lithological descriptions. Despite these limitations, the models provided valuable insights into dam decommissioning planning and risk assessment. The methodology is transferable to other tailings storage facilities and can be enhanced with higher-resolution geophysical systems and synchronized data acquisition.



#### INTRODUCTION

The characterization of tailings in mining dams is a critical step for ensuring structural safety, environmental compliance, and effective decommissioning planning. In recent years, the integration of geophysical data with geotechnical investigations has emerged as a powerful approach to improve subsurface understanding, especially when combined with machine learning techniques. This study presents a proof-of-concept (PoC) developed for a tailings dam located in the Iron Quadrangle region of Brazil. The main objective was to classify the tailings within the reservoir using a combination of airborne electromagnetic (AEM) data, ground-based geophysical surveys, and geotechnical borehole data. The project aimed to delineate geological interfaces, estimate the spatial distribution of different types of tailings, and assess associated uncertainties through supervised machine learning models.

### **METHODOLOGY**

#### **Data Sources**

This study integrated a wide range of geophysical, geotechnical, and topographic datasets. AEM data were acquired between November and December 2020 using a helicopter-towed, frequency-domain RESOLVE system. The survey used 25-meter line spacing in the north-south direction with 250-meter crosslines in the east-west direction, and a nominal altitude of 63 meters. The system included six coil pairs, magnetometers, GPS, and altimeters. The geophysics data provider generated models of electrical resistivity and magnetic susceptibility using a joint 3D inversion (Scholl and Miorelli 2019). The model grid had 12 m horizontal resolution and 4 m vertical resolution.

Ground-based geophysical surveys were conducted between 2023 and 2024 and included Electrical Resistivity Tomography (ERT), with multiple surveys using electrode spacing ranging from 1 to 10 meters and reaching maximum depths of 12 to 80 meters; Multichannel Analysis of Surface Waves (MASW), performed on the southern dike and producing S-wave velocity models up to 25 meters deep; and Horizontal-to-Vertical Spectral Ratio (HVSR), for point-based estimates of bedrock depth.

Geotechnical borehole data included standard penetration tests (SPT), mixed drilling (SPT + rotary core drilling) and Seismic Cone Penetration (SCPTu) tests, with lithological descriptions, N-SPT values, pore pressure measurements, dissipation tests, and vane shear tests. Two digital terrain models (DTMs) were used: a 2020 raster coinciding with the AEM survey date with 1-meter resolution, and a vectorized historical model representing the pre-construction terrain. The historical DTM has known issues with accuracy and does not account for excavations that modified natural terrain. Hydrogeological data included measured piezometric time series and simulations of the water table.

### **Data Processing and Validation**

All datasets underwent extensive preprocessing and validation. Automated validation was performed on geotechnical soundings using custom scripts designed to detect duplicate or missing investigation IDs, depth inconsistencies, out-of-range values, coordinate anomalies, mismatches with terrain models, and foreign key integrity issues between meta- and depth-data tables. Further manual adjustments included verifying the georeferencing of geophysical models and adjusting Z-

coordinates of boreholes based on the 2020 DTM to correct for terrain changes and inaccurate elevation data.

Manual interpretation of target values was also a key step in the process. Lithological logs were reviewed to classify materials as either anthropogenic or natural, the latter further subdivided into residual soil, saprolite, or intact rock. Undisturbed natural terrain was identified surrounding the tailings reservoir in terrain models and satellite images. CPTU data were interpreted following the methodology proposed by Robertson (2016). Thickness of soft soil was also interpreted in CPTUs occurring in the valley downstream of the dam.

Finally, terrain attributes were computed using QGIS and SAGA GIS from a downsampled 10-m resolution DTM. Values computed include, among others, slope, wetness index, valley depth, and relative elevation. To reduce high-frequency noise and enhance the extraction of broader topographic features, a Gaussian filter with a 75-meter window was applied.

## **Modelling Workflows**

This study employed two modeling workflows. The first (interface modeling) uses an enhanced version of Lysdahl et al.'s (2022) method to predict the depth of key geological boundaries: bottom of soft soil, phreatic surface (water table), bottom of tailings deposits, natural terrain (i.e., bottom of anthropogenic material), and bottom of residual soil. Features used to support predictions included principal component analysis (PCA)-reduced AEM attributes and spatial gradients thereof, geographic coordinates (x,y,z), and terrain indices. Ensembles of 30 artificial neural networks (ANNs) implemented in *TensorFlow* were trained, the output being the mean of each ensemble's predictions. Prediction uncertainty was quantified by combining ensemble variance (epistemic) and residual error (aleatory). If ground geophysics (ERT, MASW) had sufficient geophysical contrast and depth penetration to image the targeted interface, the same prediction workflow was applied on the local geophysical model, providing additional training points for the project-wide AEM model.

The second workflow performed volumetric classification similar to Christensen et al.'s (2021) method. Two predictions were performed: one for grain size (fine, transitional, coarse) using the CPTU-derived Soil Behavior Type Index (Ic), and another for contractive versus dilative behavior. Both predictions employed random forest classifiers implemented in *scikit-learn*, supported by AEM and ERT features, spatial coordinates (x,y,z), depth, and terrain attributes. The result for each voxel was the probability of each class. Confusion matrices were used to evaluate model accuracy.

## **RESULTS AND DISCUSSION**

### **Interface Models**

The interface models developed in this study provided critical insights into the subsurface structure of the tailings dam and its reservoir. The model of the natural terrain surface (Figure 1E) revealed significant depth variations, with the deepest zones located in the northeastern portion of the reservoir. These results aligned with expectations based on geomorphological features and historical deposition patterns. However, uncertainty was higher in areas with sparse training data, particularly in the western and southwestern sectors. Variations on which subsets of features show that using

AEM data but no terrain features (Figure 1D) provide a result close to the final model (Figure 1E), a promising result for other tailings facilities having AEM data but no historical terrain model.

The bottom of tailings model (Figure 2) closely followed the natural terrain within the reservoir, as expected in upstream construction dams. Outside the reservoir, the model identified anthropogenic fills and dikes, consistent with satellite imagery and terrain modifications. The residual soil base model showed thicker layers in valley bottoms, but uncertainty increased beneath the tailings due to AEM signal attenuation and a lack of direct observations from deep geotechnical soundings.

The bottom of soft soil model (Figure 3), focused on the valley downstream of the dam, successfully identified zones of soft sediments using CPTU data. Despite the limited vertical resolution of AEM at surface (~4 m), the model reproduced large-scale trends consistent with existing interpretations.

The water table generally agreed with hydrogeological simulations, but discrepancies were observed in highland areas and near drainage structures, likely due to temporal mismatches geophysical and hydrogeological datasets and limited training data.

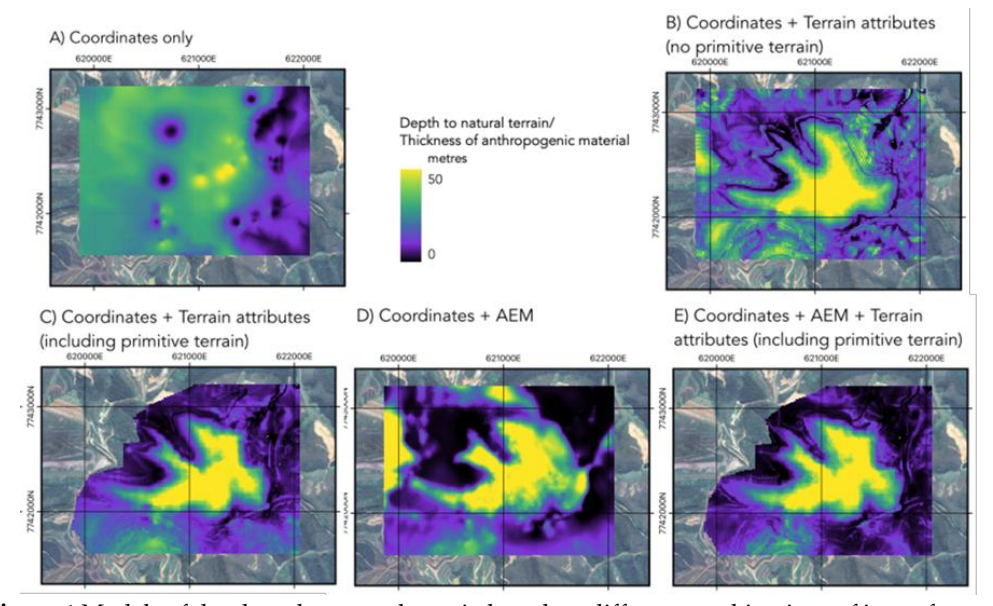
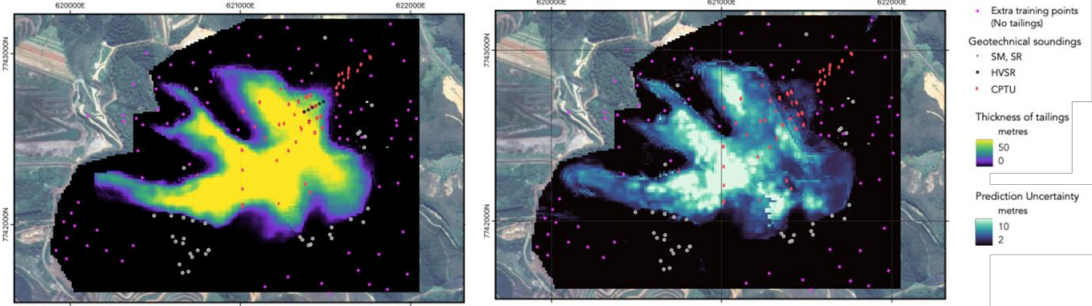
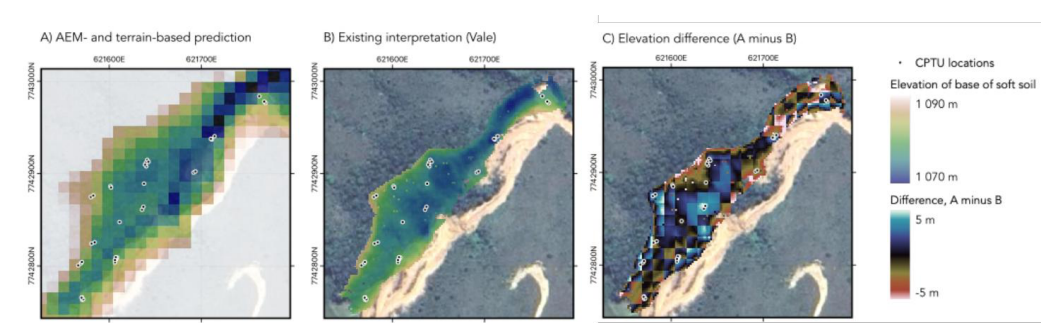


Figure 1 Models of depth to the natural terrain based on different combinations of input features



**Figure 2** Final prediction for the base of tailings interface model, based on project-wide AEM data: showing the expected thickness/depth to the base (top image) and the prediction uncertainty (bottom image)



**Figure 3** Comparison of base of soft soil models: A) AEM-based prediction; B) reference model using only geotechnical data; C) difference between the two, where positive values (blue) indicate that the AEM-based model has a higher elevation/shallower depth

#### **Volumetric Classification Models**

Two volumetric classification models were developed using CPTU-derived parameters (Figure 4). The first model, focused on grain size behavior based on Robertson's Ic, showed that fine tailings predominated the reservoir, while coarse tailings were found at depth. Transitional tailings appeared as isolated lenses. The second model classifying tailings behavior as either contractive or dilative performed well across most of the study area, with high confidence.

Both models generated probabilistic outputs, allowing for uncertainty-aware interpretation. Confusion matrices confirmed high predictive accuracy for dominant classes but showed that the first had reduced accuracy for the transitional class. This may be due to class imbalance and the narrow Ic thresholds that define the transitional class (2.4<Ic<2.6).

However, these uncertainty estimates cannot detect issues with the quality of input training targets. The presence of coarse tailings near the surface (Figure 4) likely reflects unsaturated conditions above the water table, rather than true grain size differences. The computation of Ic assuming saturated conditions is an oversimplification that should be refined in future models.

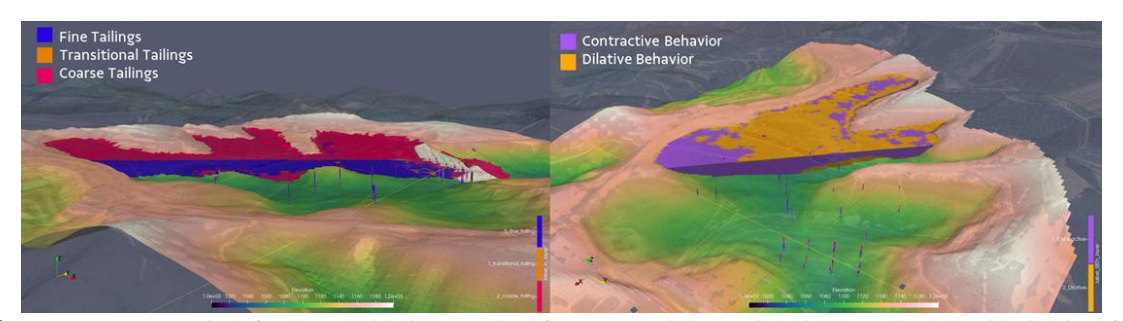


**Figure 4** Grain-size classification and behavior classification models results, showing the most likely class for each voxel

## **Modeling Challenges and Limitations**

Further models were attempted but unsuccessful. A unified model using all seven of Robertson's (2016) SBTn classes resulted in poor performance due to overlapping features, class imbalance, and limited training data—especially for transitional and mixed classes. Similarly, saprolite and intact rock were difficult to separate, partly because the training dataset relied on subjective interpretations

of saprolite versus rock by geotechnical drilling operators rather than objective metric like RQD or N-SPT. The limited depth penetration and resolution of the AEM system or a lack of a petrophysical contrast between the materials may also have been factors. These challenges highlight the need for high-resolution geophysical data, consistent field logging, and targeted sampling.

## **CONCLUSION**

This study demonstrated the feasibility and value of integrating airborne and ground-based geophysical data with geotechnical investigations using machine learning techniques to classify tailings and subsurface materials in a complex dam environment. Interface models effectively delineated key geological boundaries, including the natural terrain surface, tailings base, residual soil base, and phreatic surface, though performance varied by target depth and data availability. Volumetric classification models based on CPTU data enabled the probabilistic mapping of tailings by grain size and mechanical behavior (contractive vs. dilative). The models performed well for dominant classes, such as fine and coarse tailings, but showed limitations in transitional zones and in attempts to unify multiple classification schemes. Most importantly, by providing uncertainty estimates and probabilistic outputs, the models are more transparent about their weaknesses, allowing end-users to identify areas of high confidence and those requiring further investigation and providing a more robust foundation for risk-informed engineering decision-making.

Several challenges were encountered, including the limited resolution and penetration depth of the RESOLVE AEM system, temporal mismatches between datasets, subjectivity in lithological descriptions, inconsistent field logging, and sparse training data in critical areas—especially beneath the tailings. Despite these limitations, the models provided valuable insights and highlighted opportunities for improvement. Future efforts should focus on using higher-resolution AEM systems tailored for geotechnical applications, synchronizing data acquisition, expanding training datasets in under-sampled zones, and refining classification schemes based on updated field and laboratory data. The methodology presented is transferable to other tailings storage facilities and contributes to safer, data-driven, and more informed management practices in the mining sector.

### **ACKNOWLEDGEMENTS**

The authors would like to thank Vale S.A. and EMerald Geomodelling for making this study possible.

# **REFERENCES**

- Christensen, C.W., Harrison, E.J., Pfaffhuber, A.A. and Lund, A.K. (2021) 'A machine learning-based approach to regional-scale mapping of sensitive glaciomarine clay combining airborne electromagnetics and geotechnical data', *Near Surface Geophysics*, v19, p. 523-539. https://doi.org/10.1002/nsg.12166
- Lysdahl, A.K., Christensen, C.W., Pfaffhuber, A.A., Vöge, M., Andresen, L, Skurdal, G.H., and Panzner, M. (2022) 'Integrated bedrock model combining airborne geophysics and sparse drillings based on an artificial neural network', Engineering Geology, v.297, https://doi.org/10.1016/j.enggeo.2021.106484
- Robertson, P.K. (2016). Cone penetration test (CPT)-based soil behaviour type (SBT) classification system—an update. *Canadian Geotechnical Journal*, v. 53, n. 12, p. 1910-1927, 2016.



Scholl, C., and Miorelli, F. (2019) 'Airborne EM inversion on vertically unstructured model grids', *Exploration Geophysics*, v 51, n. 1, p. 108–121, https://doi.org/10.1080/08123985.2019.1668239